

## MODELLING OF STRATIFIED GAS-LIQUID TWO-PHASE FLOW IN HORIZONTAL CIRCULAR PIPES

**P.A.B. De Sampaio, J.L.H. Faccini**

Nuclear Engineering Institute  
Brazilian Nuclear Energy Commission (CNEN)  
21945-970, Rio de Janeiro, Brazil  
[sampaio@ien.gov.br](mailto:sampaio@ien.gov.br), [faccini@ien.gov.br](mailto:faccini@ien.gov.br)

**J. Su**

Nuclear Engineering Program, COPPE  
Universidade Federal do Rio de Janeiro  
21945-970, Rio de Janeiro, Brazil  
[sujian@con.ufrj.br](mailto:sujian@con.ufrj.br)

**Abstract.** This paper reports numerical and experimental investigation of stratified gas-liquid two-phase flow in horizontal circular pipes. The Reynolds averaged Navier-Stokes equations (RANS) with the  $\kappa$ - $\omega$  model for a fully developed stratified gas-liquid two-phase flow are solved by using the finite element method. A horizontal and smooth interface surface is assumed without considering the effects of the interfacial waves. The continuity of the shear stress across the interface is enforced with the continuity of the velocity being automatically satisfied by the variational formulation. For each given interface position and longitudinal pressure gradient, an inner iteration loop runs to solve the nonlinear equations. The Newton-Raphson scheme is used to solve the transcendental equations by an outer iteration to determine the interface position and pressure gradient for a given pair of volumetric flow rates. The interface position in a 51.2 mm ID circular pipe was measured experimentally by the ultrasonic pulse-echo technique. The numerical results were also compared with experimental results in a 21 mm ID circular pipe reported by Masala (2004). The good agreement between the numerical and experimental results indicates that the  $\kappa$ - $\omega$  model can be applied for the numerical simulation of stratified gas-liquid two-phase flow.

**Keywords.** two-phase flow, gas-liquid stratified flow, finite element method, two-equation models, horizontal pipes.

### 1. Introduction

Gas-liquid two-phase stratified flow in horizontal ducts is frequently encountered in practical applications such as nuclear reactors, oil and gas pipelines, steam generation and refrigeration equipment. The accurate prediction of pressure gradient and void fraction in gas-liquid two-phase stratified flow is of both scientific and technological interests. The 'mechanistic' model due to Taitel and Dukler (1976) has been widely used, which is a one-dimensional two-fluid model with closure relations for the wall and interfacial shear stresses calculated with single-phase flow correlations. However, the Taitel and Dukler model neglects the detailed velocity profile structure and calculates the wall and interfacial shear stresses via empirical correlations based on the averaged velocities.

With the recent advent of high-speed computers and the development of advanced turbulence models, the Computational Fluid Dynamics (CFD) techniques have been applied for the simulation of stratified gas-liquid two-phase flow. Shoham and Taitel (1984) presented one of the early two-dimensional numerical solutions of fully developed turbulent-turbulent gas-liquid flow in horizontal and inclined pipes. The gas phase was treated as bulk flow, while the liquid phase momentum equation in the bipolar coordinate system with an algebraic turbulent model was solved by using a finite difference method. Also using the bipolar coordinate system, Issa (1988) modeled stratified flow, with a smooth interface surface, but solved the axial momentum equation in both gas and liquid phases with the standard  $\kappa$ - $\epsilon$  model. Wall functions were used in the solid boundaries. The results for flow in a 25.4 mm diameter pipe agree reasonably with predictions given by the mechanistic model of Taitel and Dukler (1976). Newton and Behnia (2000) used a low Reynolds number  $\kappa$ - $\epsilon$  model that allows the solution of the turbulent-turbulent stratified flow problem without the use of empirical wall functions. The only empirical information required is the specification of damping functions in the low-Reynolds number turbulence model. The numerical results shown are in good agreement with experimental data of a 50 mm diameter pipe (Newton and Behnia, 1996) and indicate that the minor tuning of the wall damping functions performed has little effect on the results. More recently, stratified wavy two-phase flow has also been studied numerically (Meknassi et al., 2000; Newton and Behnia, 2001; Berthelsen and Ytrenhus, 2005; Ghorai and Nigam, 2006).

In this work, we solve the Reynolds averaged Navier Stokes equations (RANS) with the  $\kappa$ - $\omega$  model for a fully developed stratified gas-liquid two-phase flow using the finite element method. The  $\kappa$ - $\omega$  closure model was developed by Wilcox (2000) and is considered substantially more accurate than  $k$ - $\epsilon$  model in the near wall layers (Menter, 2003). The main drawback of the  $\kappa$ - $\omega$  model is that the  $\omega$ -equation shows a strong sensitivity to the values

of  $\omega$  in the freestream outside the boundary layer (Menter, 1992), which has largely prevented the  $\omega$  equation from replacing the  $\varepsilon$ -equation as the standard scale-equation in turbulence modeling. However, it is expected that the  $\kappa$ - $\omega$  model should have a better performance in the prediction of gas-liquid two-phase stratified flow, as no freestream boundary condition of  $\omega$  is needed in the modeling. Following Issa (1988) and Newton and Behnia (2000), a smooth and horizontal interface surface is assumed without considering the interfacial waves. The continuity of the shear stress across the interface is enforced with the continuity of the velocity being automatically satisfied by the variational formulation. The mathematical model and the variational formulation are presented in next section. The numerical techniques are then presented including the flow solver and the Newton-Raphson root-finding scheme. The numerical solution is then verified for the single-phase flow over a wide range of Reynolds number. For each given interface position and longitudinal pressure gradient, an inner iteration loop runs to solve the nonlinear equations. The Newton-Raphson scheme is used to solve the transcendental equations by an outer iteration to determine the interface position and pressure gradient for a given pair of volumetric flow rates. The numerical results are then compared with available experimental data. The experimental facility and the ultrasonic pulse-echo technique are described.

## 2. Two-phase stratified flow model

Let us consider a fully developed stratified gas-liquid two-phase flow in a horizontal pipe. In view of the symmetry of the flow with respect to the vertical plane, only a half-pipe cross-section is considered in the present model. Fig.1 shows schematically the open bounded domains occupied by the liquid and gas phases, which are denoted by  $\Omega_f$  and  $\Omega_g$ , respectively. We consider that the volumetric flow rates of the phases,  $Q_f$  and  $Q_g$ , are given.

The interface between the phases is assumed to be a horizontal plane. However, the interface position is unknown. In fact, it will be determined as a function of the given flow rates, pipe diameter and the physical properties of the liquid and gas phases. Referring to Fig.1, the gas-liquid interface is represented by  $\Gamma_{int}$ , the symmetry boundary is denoted by  $\Gamma_s$  and the pipe wall is  $\Gamma_c$ . We also define the overall open bounded domain  $\Omega = \Omega_f \cup \Omega_g \cup \Gamma_{int}$ .

The Reynolds Averaged Navier-Stokes (RANS) approach is adopted to describe the turbulent flow in both phases. For developed turbulent flow, the two-phase flow model is described by the following equations, defined within each open bounded domain  $\Omega_i$  ( $i=1$  meaning phase  $f$  and  $i=2$  meaning phase  $g$ ).

$$\nabla \cdot (A_i \nabla u) - \frac{dp}{dz} = 0 \quad (1)$$

$$\nabla \cdot (B_i \nabla \kappa) - \beta_2 \rho_i \kappa \omega + S_i = 0 \quad (2)$$

$$\nabla \cdot (C_i \nabla \omega) - \beta_1 \rho_i \omega^2 + \frac{\alpha_1 \omega}{\kappa} S_i = 0 \quad (3)$$

In the above equations the flow, with velocity  $u$ , is aligned to co-ordinate  $z$ . The kinetic energy of turbulence is represented by  $\kappa$  and the dissipation per unit turbulence kinetic energy is denoted by  $\omega$ . Because the flow is assumed to be fully developed, the same pressure gradient  $dp/dz$  is considered for both phases. Note though, that like the interface position,  $dp/dz$  is an unknown variable that will be determined as a function of the given volumetric flow rates.

Other terms appearing in Eqs. (1)-(3) are  $A_i = \mu_i + \mu_{ti}$ ,  $B_i = \mu_i + \sigma_2 \mu_{ti}$ ,  $C_i = \mu_i + \sigma_1 \mu_{ti}$  and  $S_i = A_i \nabla u \cdot \nabla u$ . The eddy viscosity for phase  $i$  is  $\mu_{ti} = \alpha_2 \rho_i \kappa / \omega$ . The  $\kappa$ - $\omega$  model parameters  $\alpha_1$ ,  $\alpha_2$ ,  $\beta_1$ ,  $\beta_2$ ,  $\sigma_1$  and  $\sigma_2$  are non-dimensional quantities. The symbol  $\nabla$  denotes the gradient operator in the cross-section analyzed. Thus, in terms of the canonical base given by the Cartesian unit vectors  $\mathbf{e}_x$  and  $\mathbf{e}_y$ , we have  $\nabla = \frac{\partial}{\partial x} \mathbf{e}_x + \frac{\partial}{\partial y} \mathbf{e}_y$ .

The model is completed by introducing boundary and interfacial conditions. The conditions on the symmetry boundary  $\Gamma_s$  are  $\nabla u \cdot \mathbf{n} = 0$ ,  $\nabla \kappa \cdot \mathbf{n} = 0$  and  $\nabla \omega \cdot \mathbf{n} = 0$ , where  $\mathbf{n}$  is the outward pointing unit vector on  $\Gamma_s$ . The pipe boundary  $\Gamma_c$  is split into  $\Gamma_{cf}$  and  $\Gamma_{cg}$ , according to the phase which is in contact with the wall. Thus, the boundary conditions on  $\Gamma_c$  are  $u = 0$ ,  $\kappa = 0$  and  $\omega = \bar{\omega}_i$  on  $\Gamma_{ci}$ , meaning that the prescribed value depends on the properties of the phase which is in contact with the pipe surface.

It is well known that  $\omega$  goes to infinity on smooth pipe walls. In order to avoid this singular behavior, we employ the same wall boundary condition implemented in the DEFT incompressible flow solver (Segal, 2006), which is given by

$$\bar{\omega}_{ci} = \frac{2 \mu_i}{\beta_0 \rho_i Y_p^2} \quad (4)$$

where  $\beta_0 = 0.072$  is a model constant and  $Y_p$  is the distance of the closest grid point to the wall.

At the interface  $\Gamma_{\text{int}}$  we impose continuity of the shear stress and consider that the interface behaves like a nearly-smooth wall (meaning that  $\kappa$  vanishes and  $\omega$  is very large but bounded). These conditions are accomplished by setting  $\sum_{i=f,g} A_i \nabla u \cdot \mathbf{n}_i = 0$ ,  $\kappa = 0$  and  $\omega = \bar{\omega}_{\text{int}}$ . We used in this work  $\bar{\omega}_{\text{int}} = 10^6 u_0/d$ , where  $d$  is the pipe diameter and  $u_0$  is a reference velocity computed using the liquid phase flow rate and the pipe cross-sectional area  $A$ , i.e.  $u_0 = Q_f/A$ .

The problem described above can be recast in variational form as follows: Find  $u \in V_u$ ,  $\kappa \in V_\kappa$  and  $\omega \in V_\omega$ , for any  $\phi \in V_\phi$  and any  $\varphi \in V_\varphi$ , such that

$$\sum_{i=f,g} \int_{\Omega_i} A_i \nabla \phi \cdot \nabla u \, d\Omega_i = - \sum_{i=f,g} \int_{\Omega_i} \phi \frac{dp}{dz} \, d\Omega_i \tag{5}$$

$$\begin{aligned} \sum_{i=f,g} \int_{\Omega_i} \phi \beta_2 \rho_i \omega \kappa \, d\Omega_i + \sum_{i=f,g} \int_{\Omega_i} B_i \nabla \phi \cdot \nabla \kappa \, d\Omega_i &= \\ = \sum_{i=f,g} \int_{\Omega_i} \phi A_i \nabla u \cdot \nabla u \, d\Omega_i & \end{aligned} \tag{6}$$

$$\begin{aligned} \sum_{i=f,g} \int_{\Omega_i} \phi \beta_1 \rho_i \omega^2 \, d\Omega_i + \sum_{i=f,g} \int_{\Omega_i} C_i \nabla \phi \cdot \nabla \omega \, d\Omega_i &= \\ = \sum_{i=f,g} \int_{\Omega_i} \phi \alpha_1 \frac{\omega}{\kappa} A_i \nabla u \cdot \nabla u \, d\Omega_i & \end{aligned} \tag{7}$$

where,

$$V_u = \{u \in H_1(\Omega), u = 0 \text{ on } \Gamma_c\} \tag{8}$$

$$V_\kappa = \{\kappa \in H_1(\Omega_f \cup \Omega_g), \kappa = 0 \text{ on } \Gamma_c, \kappa = 0 \text{ on } \Gamma_{\text{int}}\} \tag{9}$$

$$V_\omega = \{\omega \in H_1(\Omega_f \cup \Omega_g), \omega = \bar{\omega}_{ci} \text{ on } \Gamma_{ci}, \omega = \bar{\omega}_{\text{int}} \text{ on } \Gamma_{\text{int}}\} \tag{10}$$

$$V_\phi = \{\phi \in H_1(\Omega), \phi = 0 \text{ on } \Gamma_c\} \tag{11}$$

$$V_\varphi = \{\varphi \in H_1(\Omega_f \cup \Omega_g), \varphi = 0 \text{ on } \Gamma_c, \varphi = 0 \text{ on } \Gamma_{\text{int}}\} \tag{12}$$

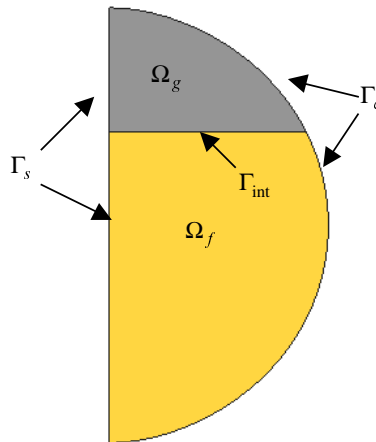


Figure 1. Schematic representation of the pipe cross-section.

Note that the problem described above is not closed: the pressure gradient  $dp/dz$  and the interface position  $y_{\text{int}}$ , which ultimately defines the domains  $\Omega_f$  and  $\Omega_g$ , are unknown. The equations that close the model come from the requirement to meet the imposed flow rates  $Q_f$  and  $Q_g$ , i.e.,

$$Q_f = 2 \int_{\Omega_f} u d\Omega \quad (13)$$

$$Q_g = 2 \int_{\Omega_g} u d\Omega \quad (14)$$

### 3. Numerical techniques

The solution is obtained by using an iterative process. This combines two numerical techniques. The first is an external Newton-Raphson method aimed to adjust  $y_{\text{int}}$  and  $dp/dz$ , in order to satisfy Eqs. (13, 14). The second, which we call the flow solver, runs internally and involves the finite element solution of the non-linear problem given by Eqs. (5-7), for given values of  $y_{\text{int}}$  and  $dp/dz$ .

#### 3.1. Newton-Raphson scheme

Let us suppose that, for a given pair of  $y_{\text{int}}$  and  $dp/dz$ , we have a numerical method to approximate and solve Eqs. (5-7) (such a method will be described in the next section). Then we can compute the mismatch of the flow rates obtained for a given pair of  $y_{\text{int}}$  and  $dp/dz$  and the flow rates  $Q_f$  and  $Q_g$  imposed as problem data. The mismatch functions are

$$F\left(\frac{dp}{dz}, y_{\text{int}}\right) = 2 \int_{\Omega} u d\Omega - Q_f \quad (15)$$

$$G\left(\frac{dp}{dz}, y_{\text{int}}\right) = 2 \int_{\Omega} u d\Omega - Q_g \quad (16)$$

Introducing  $x = dp/dz$  and  $y = y_{\text{int}}$  to simplify notation, we can formulate the problem as a system of two non-linear equations whose solution  $(x, y)$  must satisfy

$$F(x, y) = 0 \quad (17)$$

$$G(x, y) = 0 \quad (18)$$

The Newton-Raphson method is used to compute the solution of the above non-linear system. If  $x^n, y^n$  is the present approximate solution, the next approximation is computed according to

$$x^{n+1} = x^n + \frac{\left(G \frac{\partial F}{\partial y} - F \frac{\partial G}{\partial y}\right)^n}{\left(\frac{\partial F}{\partial x} \frac{\partial G}{\partial y} - \frac{\partial G}{\partial x} \frac{\partial F}{\partial y}\right)} \quad (19)$$

$$y^{n+1} = y^n + \frac{\left(F \frac{\partial G}{\partial x} - G \frac{\partial F}{\partial x}\right)^n}{\left(\frac{\partial F}{\partial x} \frac{\partial G}{\partial y} - \frac{\partial G}{\partial x} \frac{\partial F}{\partial y}\right)} \quad (20)$$

Therefore, starting from an initial guess, the above equations provide an iterative algorithm to obtain a solution of the non-linear system given by Eqs. (17,18). The iterations proceed until the mismatch functions  $F$  and  $G$  are considered to be negligibly small.

Before we proceed, note that we need to compute derivatives of  $F$  and  $G$  with respect to the unknowns  $x$  and  $y$ . These derivatives are evaluated numerically, by using small increments  $\Delta x$  and  $\Delta y$ . To compute them we have to evaluate  $F$  and  $G$  at  $(x^n + \Delta x, y^n)$ ,  $(x^n, y^n + \Delta y)$  and  $(x^n, y^n)$ . This means that we need to solve Eqs. (5)-(7) three times for each Newton-Raphson iteration.

### 3.2. Flow solver

Given the interface position and the pressure gradient, the finite element method is used to obtain an approximate numerical solution of Eqs. (5)-(7).

The finite element mesh used is specially designed to have a large number of horizontal lines. Thus, for a given interface position, a simple algorithm is used to find and select the mesh horizontal line that is closest to the desired interface position. Then the finite element mesh is adjusted so that the selected horizontal line is moved to the desired interface location. The finite elements above the interface are associated to phase  $g$  whilst the elements below it are associated to phase  $f$ .

We use linear triangular finite elements to approximate the flow variables as  $\hat{u} = N_p u_p$ ,  $\hat{\kappa} = N_p \kappa_p$  and  $\hat{\omega} = N_p \omega_p$ , where  $N_p$  are the finite element linear shape functions and  $u_p$ ,  $\kappa_p$  and  $\omega_p$  are the corresponding nodal values.

Because Eqs. (5)-(7) are non-linear, an iterative process is required. Thus, the velocity field is updated by solving the discretized counterpart of Eq. (5), i.e.,

$$\sum_{i=f,g} \int_{\Omega_i} A_i \nabla N_q \cdot \nabla \hat{u}^{n+1} d\Omega_i = - \sum_{i=f,g} \int_{\Omega_i} N_q \frac{dp}{dz} d\Omega_i \quad \forall \text{ free } u_q^{n+1} \quad (21)$$

next, the kinetic energy is updated  $\hat{\kappa}^{n+1}$  solving

$$\begin{aligned} \sum_{i=f,g} \int_{\Omega_i} N_q \beta_2 \rho_i \hat{\omega}^n \hat{\kappa}^{n+1} d\Omega_i + \sum_{i=f,g} \int_{\Omega_i} B_i \nabla N_q \cdot \nabla \hat{\kappa}^{n+1} d\Omega_i = \\ = \sum_{i=f,g} \int_{\Omega_i} N_q A_i \nabla \hat{u}^{n+1} \cdot \nabla \hat{u}^{n+1} d\Omega_i \quad \forall \text{ free } \kappa_q^{n+1} \end{aligned} \quad (22)$$

and finally, the new  $\hat{\omega}^{n+1}$  is obtained solving

$$\begin{aligned} \sum_{i=f,g} \int_{\Omega_i} N_q \beta_1 \rho_i \hat{\omega}^n \hat{\omega}^{n+1} d\Omega_i + \sum_{i=f,g} \int_{\Omega_i} C_i \nabla N_q \cdot \nabla \hat{\omega}^{n+1} d\Omega_i = \\ = \sum_{i=f,g} \int_{\Omega_i} N_q \alpha_1 \frac{\hat{\omega}^n}{\hat{\kappa}^n} A_i \nabla \hat{u}^{n+1} \cdot \nabla \hat{u}^{n+1} d\Omega_i \quad \forall \text{ free } \omega_q^{n+1} \end{aligned} \quad (23)$$

Eqs. (21)-(23) lead to symmetric systems of algebraic equations, which are solved using a Jacobi-preconditioned conjugate gradient method.

The process of solving Eqs. (21)-(23) is repeated until a prescribed convergence criterion is satisfied.

### 3.3. Code verification

In order to check the turbulence model employed and the computer implementation of the code, we have tested our procedures in a single phase problem, where we can compare our prediction for friction factor with corresponding theoretical and correlated experimental data.

This rather simple test consists of assigning the same fluid properties and flow rates for both phases. We have also relaxed the interface conditions on  $\kappa$  and  $\omega$ . This permits mimicking a single-phase computation using our two-phase computer code. As expected, the Newton-Raphson method found that the interface position is at the middle of the pipe, at  $y_{\text{int}} = 0$ . The Newton-Raphson converged value for  $dp/dz$  was used to compute the friction factor obtained in our numerical experiment.

Figure 2 presents a comparison of our data with the theoretical friction factor for laminar flow and with the friction factor predicted by Colebrook correlation for turbulent flow in a hydrodynamically smooth circular pipe. Note that our

results compare well with the expected values for both laminar and turbulent flow, although the friction factor was over-estimated in the transition region.

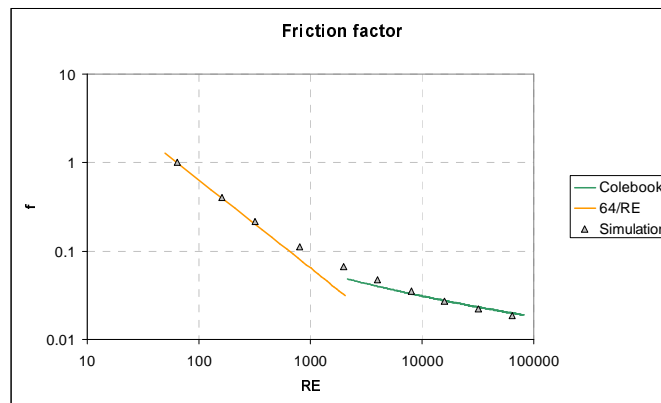


Figure 2. Single-phase friction factor as a function of the Reynolds number: comparison of numerical simulation with expected values.

#### 4. Experimental techniques

The experiments reported in this paper were conducted in the two-phase test rig of the Nuclear Engineering Institute (IEN). The rig consists of a venturi mixer, a horizontal tube, an expansion reservoir and an air water separation tank. The horizontal tube is a 5 m long stainless steel 316 with an inner diameter of 0.0512 m, followed by a short tube 0.6 m long transparent extruded acrylic with the same inner diameter. A detailed description of the test section can be found in Faccini et al. (2004). The basic principles to measure liquid height in horizontal stratified two-phase flow are illustrated in Fig. 3. The ultrasound pulse discharged from an emitter-receiver transducer, placed at bottom of tube, will be transmitted through the water and then reflected back to the same transducer from air-water or tube wall-water interfaces. Typical ultrasound signals acquired over a period of time and plotted as waveforms are shown in Fig.4 where  $\Delta t_1$  is the transit time of the ultrasound pulse through the tube wall and  $\Delta t_2$  is the transit time into the water. By measuring  $\Delta t_2$  and knowing the sound velocity through water, the water film height can be calculated very accurately by

$$h_L = c_w \frac{\Delta t_2}{2} \tag{24}$$

where  $h_L$  is the water thickness e  $c_w$  is the water sound velocity (at a given temperature).

The transit time signals are acquired during a period of 50 seconds, stored in a computer and then the results are obtained calculating the interval time between two successive echoes.

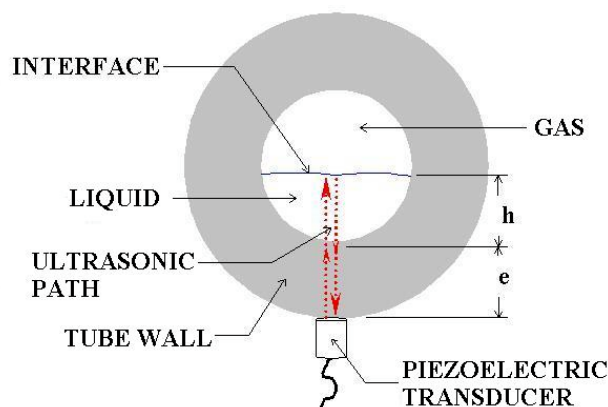


Figure 3. Schematic of liquid height measurement in stratified gas-liquid flow by ultrasonic pulse-echo technique.

The minimum  $h_L$  can be estimated approximately by the water sound velocity divided by the transducer frequency and the ultrasonic resolution is given by the transducer wavelength.

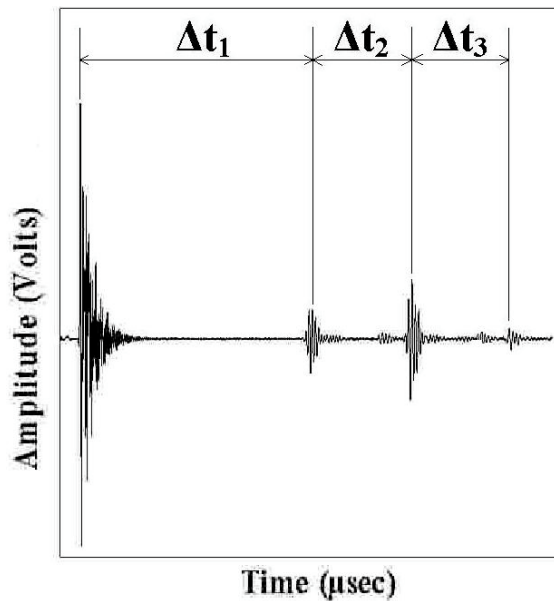


Figure 4. Typical ultrasonic signals.

### 5. Numerical and experimental results

In this section we present results for the interface position  $y_{int}$  at various flow conditions, comparing the numerical and experimental data obtained at IEN and the experiments performed by Masala (2004) at McMaster University. We have also compared our data with results obtained using the model of Taitel & Dukler (1976). The flow rates and pipe diameters used in the experiments and numerical computations are presented in Table 1.

Table 1. Flow rates and pipe diameters ( $d$ ) for the cases analyzed.

	CASE	Pipe Diam. ( $d$ ) (mm)	$Q_g$ (m <sup>3</sup> /h)	$Q_f$ (m <sup>3</sup> /h)
IEN	A	51.2	1.0	0.6
	B	51.2	2.0	0.6
	C	51.2	4.0	0.6
	D	51.2	6.0	0.6
McMaster	E	21.0	0.3	0.024
	F	21.0	0.3	0.061
	G	21.0	0.3	0.090
	H	21.0	0.3	0.121

We have performed numerical simulations for all the cases presented in Table 1. Figure 5 shows a typical result of mesh, velocity and kinetic energy. Additionally, experimental results have been obtained for cases A to D.

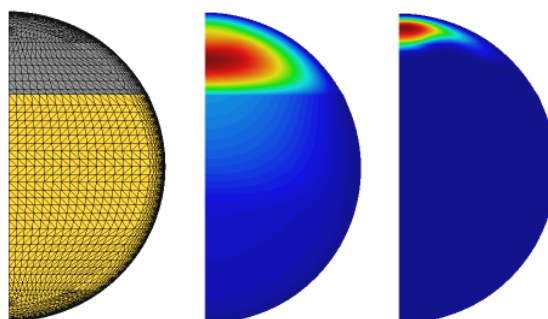


Figure 5. Mesh, velocity and turbulent kinetic energy for case A.

Figure 6 shows typical pictures taken with a high-speed camera during the IEN experiments. Despite the fact that the interfaces shown in Fig.6 are located in the upper part of the horizontal tube, it can be observed that the flow regime is stratified for the flow rates considered. Note that the model idealization depicted in Fig.1 has a better match with the flow pattern presented in Fig. 6(a) than with that shown in Fig. 6(b). A wavy interface such as that observed in Fig. 6(b)

may require non-smooth interfacial conditions in order to obtain better results from the numerical model. This will be investigated in a future work.

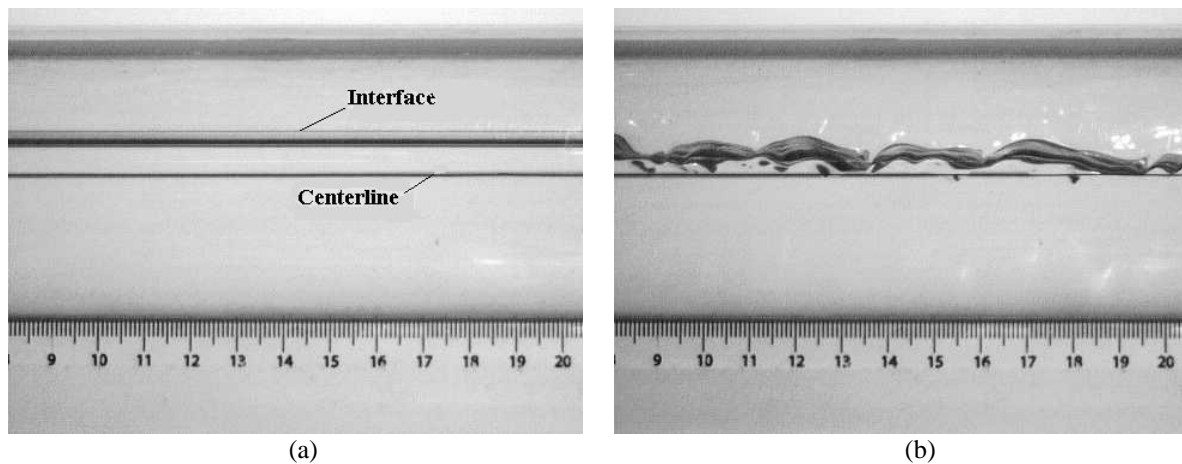


Figure 6. Stratified flow in the horizontal tube: a)  $Q_f = 0.6 \text{ m}^3/\text{h}$  and  $Q_g = 1.0 \text{ m}^3/\text{h}$ ; b)  $Q_f = 0.6 \text{ m}^3/\text{h}$  and  $Q_g = 6.0 \text{ m}^3/\text{h}$ .

Figure 7 shows the non-dimensionalized results for the interface position  $y_{\text{int}}/d$  as a function of volumetric quality  $Q_g/(Q_f + Q_g)$ , comparing the present simulation with the McMaster experiments performed by Masala (2004) and with numerical predictions obtained using the model of Taitel and Dukler (1976). Figure 8 shows similar results, this time comparing the present simulation with the experiments performed at IEN. Figures 7 and 8 show that the results of the present simulation are in reasonable agreement with both sets of experimental data and the predictions of the Taitel and Dukler model.

It is interesting to note that Masala’s experiments, for volumetric qualities higher than 0.80, have at least one of the phases undergoing transition. As we have noticed in the single-phase simulation test, the numerical model overestimates the friction factor at transition. This may explain some discrepancy observed between the present simulation results and Masala’s experiments on that volumetric quality range.

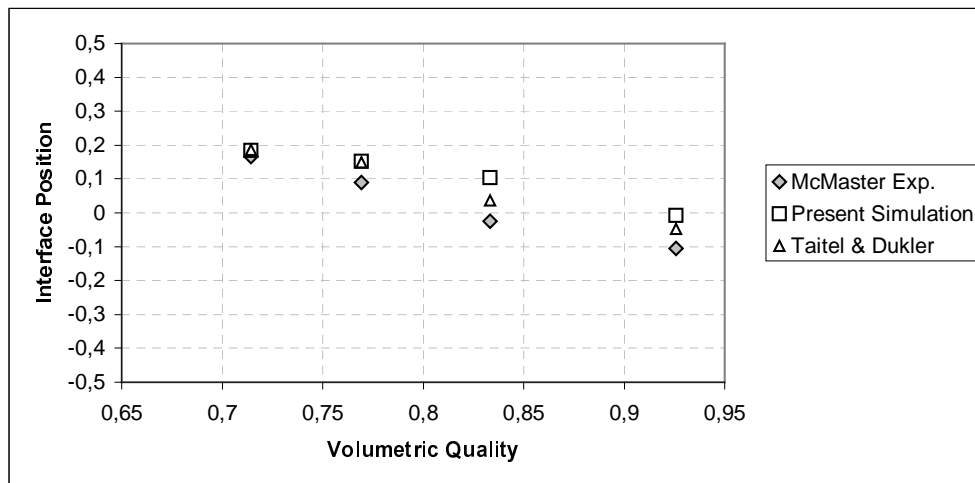


Figure 7. Non-dimensional interface position as a function of the volumetric quality: comparison of present simulation with experiments performed at McMaster University and numerical results from the Taitel & Dukler model.

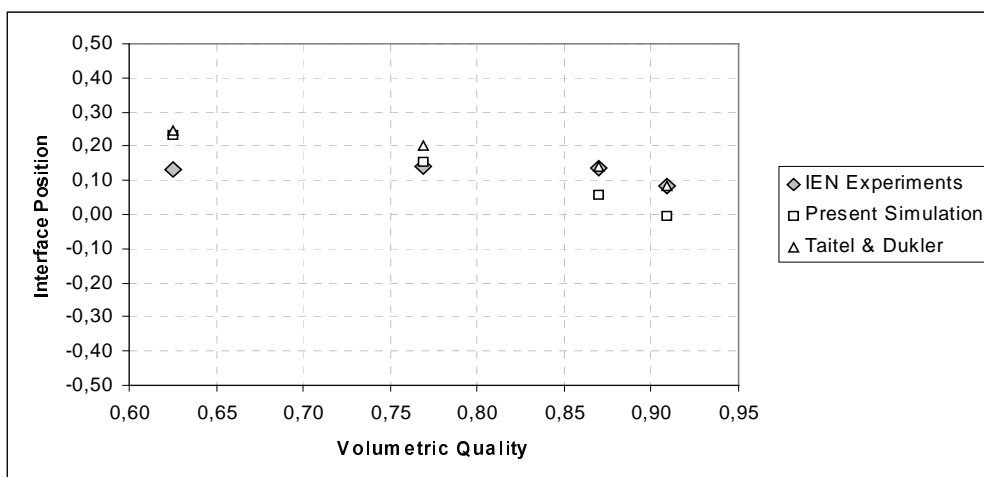


Figure 8. Non-dimensional interface position as a function of the volumetric quality: comparison of present simulation with experiments performed at IEN and numerical results from the Taitel & Dukler model.

## 6. Conclusions

In this paper we proposed physical and numerical models for stratified two-phase flows in horizontal pipes, comparing results with experimental data obtained at IEN and with those obtained by Masala (2004). We have also compared our simulation data with those obtained using the model of Taitel and Dukler (1976). The results indicate that the  $\kappa - \omega$  model is suitable for the numerical simulation of such flows. However, a better understanding on how to impose interfacial values for  $\kappa$  and  $\omega$  is needed before we can expect to obtain better agreement with experimental data of stratified wavy two-phase flow.

The computational code is being parallelized to run on a Beowulf type cluster. It is expected that with a parallel version of the code we will be able to re-calculate the cases presented here in much finer meshes, with possible improvement of the quality of the numerical results.

## 7. Acknowledgments

J.L.H. Faccini is grateful to IAEA for the donation of the instrumentation, and to Silvia B.G. Cesar for technical assistance. P.A.B de Sampaio acknowledges the support of CNPq grant 301045/2003-8. J. Su acknowledges the support of CNPq and FAPERJ.

## 8. References

- P.A. Berthelsen, T. Ytrehus, Calculation of stratified wavy two-phase flow in pipes, *Int. J. Multiphase Flow*, 31, 571-592, 2005.
- S. Ghorai, K.D.P. Nigam, CFD modeling of flow profiles and interfacial phenomena in two-phase flow in pipes, *Chem. Eng. Processing*, 45, 55-65, 2006.
- J.L.H. Faccini, J. Su, G.D. Harvel, J.S. Chang, An advanced ultrasonic technique for flow and void fraction measurements of two-phase flow, in *Proceedings of ICONE12*, Arlington, Virginia, April 25-29, 2004.
- Masala, T., 2004, "High-Speed Ultrasonic Pulse-echo System for Two-Phase Flow Measurements, M.Sc. Thesis, McMaster University, Hamilton, Canada.
- R.I. Issa, Prediction of turbulent, stratified, two-phase flow in inclined pipes and channel, *Int. J. Multiphase Flow*, 14, 141-154, 1988.
- F. Mekkassi, R. Benkirane, A. Liné, L. Masbernat, Numerical modeling of wavy stratified two-phase flow in pipes, *Chem. Eng. Sci.*, 55, 4681-4697, 2000.
- F.R. Menter, Influence of freestream values of on  $k-\omega$  turbulence model predictions, *AIAA J.*, 30, 1992.
- F.R. Menter, M. Kunz, E. Langtry, Ten years of industrial experience with the SST turbulence model, in K. Hanjalic, Y. Nagano and M. Tummers (eds.), *Turbulence, Heat and Mass Transfer 4*, 2003.
- C.H. Newton, M. Behnia, Estimation of wall shear stress in horizontal gas-liquid stratified flow, *AIChE J.*, 42, 2369-2373, 1996.
- C.H. Newton, M. Behnia, Numerical calculation of turbulent stratified gas-liquid pipe flows, *Int. J. Multiphase Flow*, 26, 327-337, 2000.
- C.H. Newton, M. Behnia, A numerical model of stratified wavy gas-liquid pipe flow, *Chem. Eng. Sci.*, 56, 6851-6861, 2001.

- G. Segal, M. Zijlema, R. van Nooyen, C. Moulinec, User Manual of the DEFT incompressible flow solver, Delft Univ. of Technology, available at [ta.twi.tudelft.nl/isnas/usermanual.pdf](http://ta.twi.tudelft.nl/isnas/usermanual.pdf).
- O. Shoham, Y. Taitel, Stratified turbulent-turbulent gas-liquid flow in horizontal and inclined pipes, *AIChE J.*, 30, 377-385, 1984.
- Y. Taitel, A.E. Dukler, Model for predicting flow regime transitions in horizontal and near horizontal gas-liquid flow, *AIChE*, 22, 591-595, 1976.
- D.C. Wilcox, *Turbulence Modelling for CFD*, 2<sup>nd</sup> Edition, DCW Industries, USA, 2000.

## **9. Copyright Notice**

The authors are the only responsible for the printed material included in this paper.